JACS
JOURNAL OF THE AMERICAN CHEMICAL SOCIETY

Communication

pubs.acs.org/JACS

DNA Crystals as Vehicles for Biocatalysis

Chun Geng and Paul J. Paukstelis*

Department of Chemistry & Biochemistry, Center for Biomolecular Structure and Organization, and Maryland NanoCenter, University of Maryland, College Park, Maryland 20742, United States

Supporting Information

ABSTRACT: Here we demonstrate that protein enzymes captured in the solvent channels of three-dimensional DNA crystals are catalytically active. Using RNase A as a model enzyme system, we show that crystals infused with enzyme can cleave a dinucleotide substrate with similar kinetic restrictions as other immobilized enzyme systems. This new vehicle for immobilized enzymes, created entirely from biomolecules, opens possibilities for developing modular solid-state catalysts that could be both biocompatible and biodegradable.

DNA has proved to be a successful material for the self-assembly of nanoscale structures in two and three dimensions because of its inherent programmability and predictable structural features.[1] One of the original[2] and ongoing goals of the DNA nanotechnology field has been the rational design of periodic three-dimensional (3D) DNA arrays, or crystals.[3] DNA crystals have been envisioned as self-assembling porous solids that could be used as molecular scaffolds for the determination of protein structures, as templates for 3D molecular electronics,[4] or as zeolite-like materials for separations and catalysis.[5] In this study, we show that a protein enzyme encapsulated in the solvent channels of a DNA crystal is capable of performing catalysis. The encapsulated enzyme has kinetic properties consistent with those of other immobilized enzymes[6] and represent a solid-state biomolecular catalyst composed entirely of biological molecules.

The previously described DNA crystals used in this study were designed to have both canonical B-form DNA segments and noncanonical homopurine base-paired regions (Figure 1A).[7] The crystals contain axially distinct solvent channels that run through the crystal in multiple directions. Down the sixfold crystallographic symmetry axis these channels are ∼9 nm in diameter (Figure 1B), and previous work showed that proteins with molecular weights of 14−45 kDa could be incorporated into these channels while larger proteins could be excluded from the crystal interior.[8] Building on these observations, we have examined the catalytic activity of enzymes encapsulated within the crystals' solvent channels while distinguishing this activity from any enzyme free in solution.

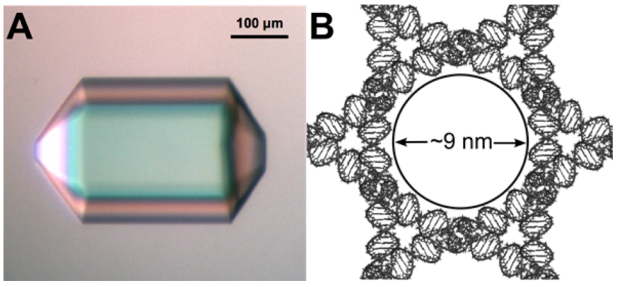

Figure 1. Three-dimensional DNA crystals. (A) Picture of a representative crystal used in this study. (B) The crystals contain channels ∼9 nm in projection that run down the sixfold symmetry axis.

We chose bovine RNase A as a model enzyme for these studies. RNase A has a molecular weight of ∼14 kDa,[9] placing it within the range of proteins that can be absorbed into the channels of the crystals. It is also highly stable under a variety of reaction conditions and can be assayed using a wide variety of substrates.[10] For this study, we used a quenched fluorescent rUA dinucleotide similar to those used in previous studies.[11] Briefly, the dinucleotide contained 5′-dabcyl and 3′-fluorescein moieties to enable fluorescence release upon cleavage of the scissile phosphodiester linkage (Scheme 1). Importantly, RNase A is also potently inhibited by the protein ribonuclease inhibitor (RI) through tight interactions with a femtomolar dissociation constant.[12] With a molecular weight of ∼50 kDa, RI is also significantly larger than RNase A and slightly above the size limit of proteins that were detected in the crystal interior. However, to avoid potential inhibition of RNase A by RI inside the crystals, we constructed a 90 kDa MBP−RI fusion protein (see the Supporting Information) that was used interchangeably with commercially available RI.

DNA crystals were loaded with RNase A by soaking for 4 days in 44 mg/mL RNase A at 4 °C. The crystals were washed extensively with buffer before being incubated with RI or MBP−RI prior to initiation of reactions. Pilot experiments using washed and dissolved crystals established the amount of inhibitor necessary to inhibit all of the RNase present in a medium-sized crystal (defined here as being ∼200 μm across the hexagonal base). All of the activity assays used 4 times this amount of inhibitor to ensure its excess. Immunoblot analysis from several crystals indicated that typical crystals contained ∼20 ng of RNase A (Figure S1 in the Supporting Information).

The RNase A activity of loaded crystals was monitored in several ways. Prepared crystals were transferred directly to a low-volume fluorescence cuvette containing reaction buffer and substrate. Fluorescence accumulation was monitored over time without agitation (Figure 2A). For some crystals, we observed anomalous peaks (Figure S2), which we attributed primarily to the crystal being in the cuvette light path. Following the initial 3

Received: March 7, 2014
Published: May 16, 2014

   dx.doi.org/10.1021/ja502356m | J. Am. Chem. Soc. 2014, 136, 7817−7820

Scheme 1. RNase A-Infused DNA Crystals as Solid-State Catalysts

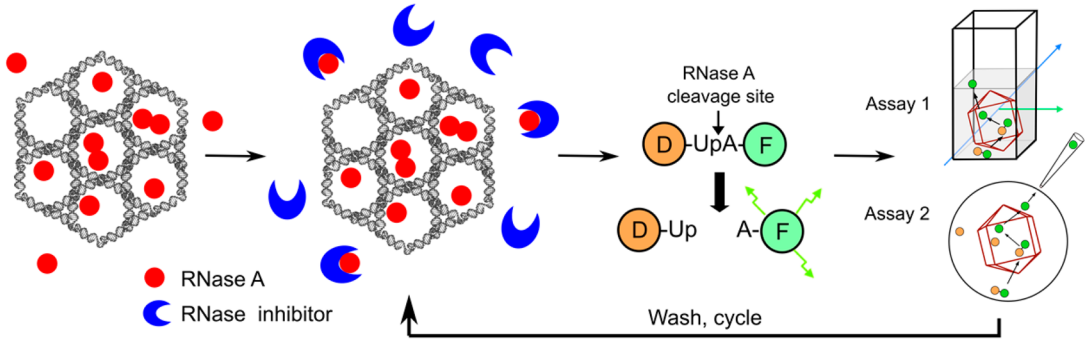

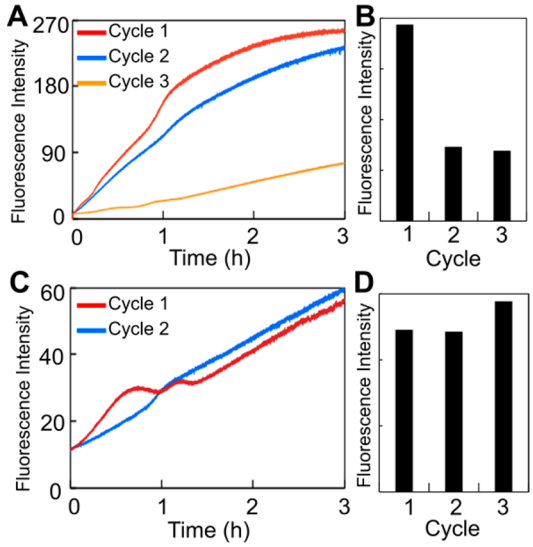

Figure 2. RNase A activity of (A, B) uncoated and (C, D) lysozyme-coated DNA crystals. Single-crystal fluorometer intensities versus time (assay 1) are shown in A and C. Bulk solution fluorescence intensities at a single time point (60 min) for different crystals (assay 2) are shown in B and D. Only two cycles are shown in C.

h reaction, crystals were reused by washing for at least 30 min to remove substrates and products, incubation with fresh inhibitor, and transfer to new reaction buffer. Similar profiles were observed for multiple cycles but with decreased overall fluorescence, presumably due to the loss or inactivation of RNase A during the washing steps. To avoid anomalous fluorescence peaks and to mitigate breaking or cracking of crystals when they were removed from the cuvette, we used assay 2 (Scheme 1). Similar results were obtained using this assay when the crystals were incubated under the same conditions, but aliquots of the reaction buffer were removed from around the crystals at various time points and the fluorescence was measured (Figure 2B). There was little change in fluorescence intensity of the individual time points over 20 min (Figure S3), indicating that any RNase A released into the solution during the assay or washing steps was effectively bound by the inhibitor.

To improve the reusability of the RNase A-infused crystals, we developed a coating technique to prevent the loss of enzyme. Washed crystals were incubated with 30 mg/mL hen egg-white lysozyme solutions for 5 min and then transferred to fresh buffer containing 2% glutaraldehyde for 20 min. Western blot analysis did not show higher-molecular-weight RNase A (Figure S4), indicating that under these conditions there was little intermolecular cross-linking of the enzyme. In both of the assay methods described above, RNase activity profiles for the coated crystals were maintained over sequential cycles (Figure 2C,D) with up to 4 days between cycles (Figure S5). Presumably, glutaraldehyde cross-links lysozyme molecules that are associated with the crystal surface and those that have entered the crystal solvent channels. This likely leads to the formation of high-molecular-weight aggregates in or around the crystal apertures that are not readily dissociated by washing. We cannot rule out cross-linking of individual lysozyme molecules or aggregates directly to nucleobases of the DNA strands, leading to solvent channel occlusion.

Having crystals that retained activity over multiple cycles allowed us to attempt to determine steady-state kinetic parameters for the encapsulated enzymes. Single lysozyme-coated crystals were incubated at seven different substrate concentrations sequentially. Aliquots of the reactions were taken at various time points and used to determine initial reaction velocities. Multiple crystals showed good agreement, and little difference was observed when the reaction series were done with ascending or descending substrate concentrations. Plots of initial velocity versus substrate concentration showed nonhyperbolic saturation kinetics in the measurable substrate range (Figure 3). This non-Michaelis–Menten behavior is consistent with that of other examples of immobilized[6] enzymes and can be attributed to the significant mass-transfer effects resulting from both external and internal diffusion of substrates and products in such large crystals. These effects can be mitigated at high substrate concentration,[6c] but in this case,

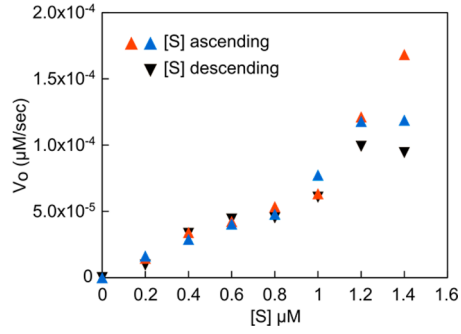

Figure 3. Non-Michaelis–Menten kinetics of RNase A-infused crystals. Initial velocities determined from seven substrate concentrations for three independent crystals are plotted versus substrate concentration. These show nonhyperbolic substrate dependence. Similar results were obtained with ascending or descending substrate concentrations, with the most variability at the highest concentration.

dx.doi.org/10.1021/ja502356m | J. Am. Chem. Soc. 2014, 136, 7817–7820

testing higher substrate concentrations proved intractable because of the difficulty in obtaining early time points in the linear range. Importantly, because the free enzyme does follow Michaelis–Menten kinetics,[13] this result further supports the conclusion that the observed dinucleotide cleavage events occur inside the crystal.

Finally, we used confocal microscopy to directly visualize the release of fluorescence signal from the crystal (Figure 4).

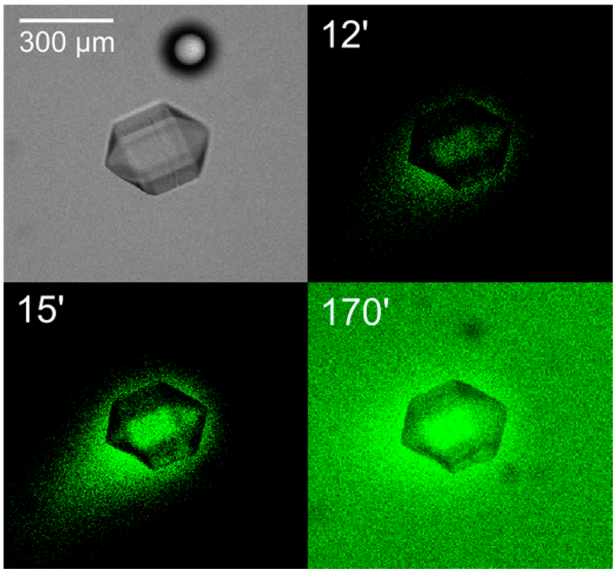

Figure 4. Confocal microscopy of RNA substrate cleavage by a DNA crystal. RNA substrate (final concentration, 2 μM) was added to a single RNase A-infused DNA crystal, and the fluorescence was monitored by confocal microscopy over time.

Substrate was added to standard reaction conditions containing the crystal, and multiple planes through the crystal were imaged over time. Depending on the substrate concentration, we observed detectable localized fluorescence release within 12 min that was initially most intense around the periphery of the crystal. However, within minutes the interior fluorescence had achieved comparable levels. This is consistent with the encapsulated enzymes closest to the crystal periphery being likely to contact substrate first, while diffusion effects limit substrate accessibility to the more deeply buried enzymes. Interestingly, even at late time points, there was greater fluorescence apparent at the sixfold ends of the crystal periphery, possibly indicating preferential product release from the much larger crystal pores present down this axis (in projection, ~6300 Å^2 parallel to the sixfold axis versus ~2700 Å^2 perpendicular to it).

The development of solid-state enzymatic catalysts in a DNA framework may have a number of advantages over other crystal-based biocatalysis systems.[6c−f] The most significant of these may be the potential to develop modular catalysts by incorporating different enzymes into the crystal solvent channels. A natural extension of these types of modular crystals would be the introduction of multiple enzymes to perform sequential reactions. The observed kinetic restrictions are a problem common to cross-linked protein crystals and the crystals described here. Solutions to this problem with cross-linked protein crystals include reducing the carrier size and decreasing the enzyme loading density. This may be achieved with DNA crystals through controlled growth conditions or modified enzyme soaking conditions. It may be necessary in some cases to crystallize the DNA in the presence of the enzymes to improve the incorporation yield, particularly when the enzyme size approaches the occlusion limit of the solvent channels. Similar to cross-linked protein crystals,[6c−e] these DNA crystals are composed entirely of biomolecules, making them biodegradable and potentially biocompatible for environmental or biomedical applications.

■ ASSOCIATED CONTENT

Ⓢ Supporting Information

Detailed experimental methods and Figures S1–S5. This material is available free of charge via the Internet at http://pubs.acs.org.

■ AUTHOR INFORMATION

Corresponding Author

paukstel@umd.edu

Notes

The authors declare no competing financial interest.

■ ACKNOWLEDGMENTS

We thank J. Hofsteenge for the generous gift of the RI ORF, L. Li and Z. Xiao for suggestions on Western blotting, and G. Lorimer for fluorometer usage.

■ REFERENCES

(1) (a) Seeman, N. C. *Nature* **2003**, *421*, 427. (b) Ouldridge, T. E.; Hoare, R. L.; Louis, A. A.; Doye, J. P.; Bath, J.; Turberfield, A. J. *ACS Nano* **2013**, *7*, 2479. (c) Gait, M. J.; Komiyama, M.; Seeman, N. C.; Seitz, O.; Micklefield, J.; Liu, D. R. *Org. Biomol Chem.* **2013**, *11*, 2058. (d) Chandran, H.; Rangnekar, A.; Shetty, G.; Schultes, E. A.; Reif, J. H.; LaBean, T. H. *Biotechnol. J.* **2013**, *8*, 221. (e) Rothemund, P. W. *Nature* **2006**, *440*, 297. (f) Winfree, E.; Liu, F.; Wenzler, L. A.; Seeman, N. C. *Nature* **1998**, *394*, 539. (g) Liu, D.; Wang, M.; Deng, Z.; Walulu, R.; Mao, C. *J. Am. Chem. Soc.* **2004**, *126*, 2324. (h) Shih, W. M.; Quispe, J. D.; Joyce, G. F. *Nature* **2004**, *427*, 618. (i) Andersen, E. S.; Dong, M.; Nielsen, M. M.; Jahn, K.; Subramani, R.; Mamdouh, W.; Golas, M. M.; Sander, B.; Stark, H.; Oliveira, C. L.; Pedersen, J. S.; Birkedal, V.; Besenbacher, F.; Gothelf, K. V.; Kjems, J. *Nature* **2009**, *459*, 73. (j) Majumder, U.; Rangnekar, A.; Gothelf, K. V.; Reif, J. H.; LaBean, T. H. *J. Am. Chem. Soc.* **2011**, *133*, 3843.

(2) Seeman, N. C. *J. Theor. Biol.* **1982**, *99*, 237.

(3) (a) Sha, R.; Birktoft, J. J.; Nguyen, N.; Chandrasekaran, A. R.; Zheng, J.; Zhao, X.; Mao, C.; Seeman, N. C. *Nano Lett.* **2013**, *13*, 793. (b) Zheng, J.; Birktoft, J. J.; Chen, Y.; Wang, T.; Sha, R.; Constantinou, P. E.; Ginell, S. L.; Mao, C.; Seeman, N. C. *Nature* **2009**, *461*, 74.

(4) Robinson, B. H.; Seeman, N. C. *Protein Eng.* **1987**, *1*, 295.

(5) Ribeiro, F. R.; Alvarez, F.; Henriques, C.; Lemos, F.; Lopes, J. M.; Ribeiro, M. F. *J. Mol. Catal. A.: Chem.* **1995**, *96*, 245.

(6) (a) Pedruzzi, I.; da Silva, E. A.; Rodrigues, A. E. *Enzyme Microb. Technol.* **2011**, *49*, 183. (b) Valencia, P.; Flores, S.; Wilson, L.; Illanes, A. *Appl. Biochem. Biotechnol.* **2011**, *165*, 426. (c) Tischer, W.; Kasche, V. *Trends Biotechnol.* **1999**, *17*, 326. (d) Spiess, A.; Schlothauer, R.; Hinrichs, J.; Scheidat, B.; Kasche, V. *Biotechnol. Bioeng.* **1999**, *62*, 267. (e) Margolin, A. L.; Navia, M. A. *Angew. Chem., Int. Ed.* **2001**, *40*, 2204. (f) St. Clair, N. L.; Navia, M. A. *J. Am. Chem. Soc.* **1992**, *114*, 7314.

(7) Paukstelis, P. J.; Nowakowski, J.; Birktoft, J. J.; Seeman, N. C. *Chem. Biol.* **2004**, *11*, 1119.

(8) Paukstelis, P. J. *J. Am. Chem. Soc.* **2006**, *128*, 6794.

(9) Raines, R. T. *Chem. Rev.* **1998**, *98*, 1045.

(10) Kelemen, B. R.; Klink, T. A.; Behlke, M. A.; Eubanks, S. R.; Leland, P. A.; Raines, R. T. *Nucleic Acids Res.* **1999**, *27*, 3696.

(11) Park, C.; Kelemen, B. R.; Klink, T. A.; Sweeney, R. Y.; Behlke, M. A.; Eubanks, S. R.; Raines, R. T. *Methods Enzymol.* **2001**, *341*, 81.

(12) Klink, T. A.; Vicentini, A. M.; Hofsteenge, J.; Raines, R. T. *Protein Expression Purif.* **2001**, *22*, 174.
(13) Park, C.; Raines, R. T. *Biochemistry* **2003**, *42*, 3509.